Available online at www.sciencedirect.com
SCIENCE DIRECT
Journal of Power Sources 142 (2005) 292–297
JOURNAL OF POWER SOURCES
www.elsevier.com/locate/jpowsour

Nanocrystalline transition metal ferrite thin films prepared by an electrochemical route for Li-ion batteries

Yan-Na NuLi[a,b], Qi-Zong Qin[a,*]

[a] *Department of Chemistry, Laser Chemistry Institute, Fudan University, Shanghai 200433, PR China*
[b] *Department of Chemical Engineering, Shanghai Jiao Tong University, Shanghai 200240, PR China*

Received 5 July 2004; received in revised form 13 October 2004; accepted 15 October 2004
Available online 18 December 2004

Abstract

Nanocrystalline ferrite MFe_2O_4 (M = Cu, Ni, Co) thin films have been prepared by an electrochemical route involving cathodic electrodeposition of MFe_2 alloys and further anodization of the alloy films at room temperature. XRD measurements showed that those films are polycrystalline with spinel tetragonal structure for $CuFe_2O_4$, and cubic structure for $NiFe_2O_4$ and $CoFe_2O_4$, respectively. The uniform MFe_2O_4 films without cracks and pinholes were observed in SEM measurement, and the estimated grain average sizes of as-prepared ferrite films were about 50 nm. The electrochemical measurements showed that MFe_2O_4 thin film electrodes delivered a reversible capacity of 450–460 mAh g^{-1} at 10 μA cm^{-2} in the voltage range of 0.01–3.0 V and more than 75% reversible capacity still remained up to 100 cycles. Our results showed that MFe_2O_4 thin films could be used as promising anode materials for thin film lithium-ion batteries.

Keywords: Lithium-ion batteries; Nanocrystalline thin film; Transition metal ferrite MFe_2O_4 (M = Cu, Ni, Co)

1. Introduction

Iron based compounds have drawn much attention for their potential application to Li-ion batteries as electrode materials because of their low cost and low toxicity. Among these compounds, iron oxides such as α-Fe_2O_3 and spinel Fe_3O_4 have been thoroughly investigated as lithium intercalation electrodes previously. However, conventional crystalline iron oxides with micrometer particle sizes showed poor electrochemical characteristics in terms of electrode capacity and cycleability [1,2]. Recently, there have been some reports on the reinvestigation of electrochemical behavior of α-Fe_2O_3 with nanocrystalline structure. Tarascon and co-workers [3] carried out in situ X-ray diffraction studies on the effect of particle size on lithium intercalation into α-Fe_2O_3 and found that nanocrystalline α-Fe_2O_3 exhibited better electrochemical performance than macro-sized (>100 nm) α-Fe_2O_3. Xu and Jain [4] also reported a nanocrystalline ferric oxide Fe_2O_3 that displayed high specific capacity and excellent capacity retention upon cycling. These investigations have led to a renewed interest in using nanosized metal oxides as promising electrode materials for rechargeable Li-ion batteries.

Most of transition metal oxides MO can react with Fe_2O_3 to form ferrite MFe_2O_4. Ferrite materials have attracted considerable attention for their potential applications in the electronics industries, magnetic-optic recording devices owing to their important electrical and magnetic optical properties [5,6]. Chen and Greenblatt [7] firstly reported transition metal ferrites with spinel structure used as candidates for cathode materials of lithium batteries. Recently, Tirado and co-workers reported that spinel mixed transition metal oxides such as $NiCo_2O_4$ [8], $NiFe_2O_4$ [9] and $CoFe_2O_4$, $CuFe_2O_4$ [10] powder could be used as active anode materials for lithium-ion batteries. However, their preliminary results of $NiFe_2O_4$, $CoFe_2O_4$, $CuFe_2O_4$ electrodes showed that the reversible capacity of these anode materials dropped rapidly with poor cycleability. This is the major drawback for

* Corresponding author. Tel.: +86 21 6510 2777; fax: +86 21 6510 2777.
E-mail address: qzqin@fudan.ac.cn (Q.-Z. Qin).

0378-7753/$ – see front matter © 2004 Elsevier B.V. All rights reserved.
doi:10.1016/j.jpowsour.2004.10.015

their use in lithium ion batteries. Recently, we have prepared nanocrystalline $CoFe_2O_4$ [11], $ZnFe_2O_4$ and $Ag_xZnFe_2O_4$ [12] thin films by pulsed laser deposition (PLD) method and showed their electrochemical performance can be significantly improved compared with MFe_2O_4 bulk powder for the use of these film electrodes in lithium-ion batteries.

Besides pulsed laser deposition [11–13], dip coating [14], sputtering [15], laser ablation [16], vacuum arc evaporation [17] and sol–gel method [18] have been used to fabricate ferrites thin films. However, these methods require the film annealed at high temperature, which may result in film cracking, substrate oxidation and production of toxic gases. To overcome the difficulties arising from the high-temperature process, room temperature synthesis of metal ferrites thin films using electrochemical method has attracted much attention. Nanocrystalline ferrite MFe_2O_4 (M = Cu, Ni, Co) thin films have been prepared using a novel electrochemical route onto various conducting substrate at room temperature [19], but there is no report to examine whether these ferrite films can be used as anode material for lithium ion batteries.

In this paper, we attempt to continue our research on nanocrystalline metal ferrite films and their electrochemical performance used as anode materials for Li-ion batteries. Nanocrystalline $NiFe_2O_4$, $CoFe_2O_4$ and $CuFe_2O_4$ thin films are prepared by an electrochemical route combined with cathodic eletrodeposition of MFe_2 alloy and further anodization of the alloy films at room temperature. The improved electrochemical performances of MFe_2O_4 (M = Cu, Ni, Co) thin films resulting from their nanocrystalline structure are reported.

2. Experimental

The experimental conditions for room temperature synthesis of transition metal ferrite MFe_2O_4 (M = Cu, Ni, Co) thin films are similar to those reported by Sartale et al. [19] and described briefly as follows. The electrodeposition of MFe_2 thin films was carried out galvanostatically from a non-aqueous sulfate solutions by dissolving requisite amounts of metal sulfates in ethylene glycol. All solutions were prepared immediately before each experiment. The stainless steel substrate was used as a cathode, the counter electrode was a high-purity graphite plate, and the distance between cathode and anode was 0.5 cm. The substrate was anodically etched at a current density 2 mA cm^{-2} for 1 min before the deposition. The alloy films deposited at optimized deposition conditions were electrochemically oxidized at room temperature in 1N KOH aqueous solution, in which the deposited alloy films on stainless steel substrate and graphite were used as anode and cathode, respectively. The prepared ferrite thin films were washed with distilled water and preserved in desiccators. The optimized conditions for electrochemical preparation of MFe_2O_4 (M = Cu, Ni, Co) thin films are listed in Table 1.

The morphology and structure of the ferrite thin films were examined using an X-ray diffractometer (Bruker Analytical X-ray systems, Germany) with Cu Kα radiation. Scanning electron microscopy (Philips XL30) was used to determine the film morphology and thickness. The weight of the film was estimated from the film thickness, area and density of MFe_2O_4.

The electrochemical cells were assembled in a glove box under dry argon. Cyclic voltammetric tests were performed at room temperature using a conventional three-electrode cell, in which metallic lithium foils were used as both counter and reference electrodes, and ferrite thin film was used as a working electrode. Discharge–charge measurements were carried out using Swagelok-type cell [20] with ferrite thin film as the positive electrode and high-purity lithium metal foil as the negative electrode. The electrolyte was 1 M $LiPF_6$ dissolved in a 1:1 (w/w) mixture of ethyl carbonate (EC) and dimethyl carbonate (DMC), and a Celgard 2400 membrane as the cell separator. Cyclic voltammograms were performed using CHI660A electrochemical workstation and chronopotentiometric data were recorded using a LAND cell testing system.

3. Results and discussion

XRD patterns of as-prepared MFe_2O_4 (M = Cu, Ni, Co), thin films are shown in Fig. 1. According to the JCPDS reference (34–425), (10–325) and (3–864), the diffraction peaks at $2\theta = 35.8^\circ$, 35.6° and 35.4° can be attributed to (2 1 1) and (3 1 1) reflections of the spinel tetragonal structure for $CuFe_2O_4$, and cubic structure for $NiFe_2O_4$ and $CoFe_2O_4$, respectively. The diffraction peaks at $2\theta = 43.6^\circ$, 50.6° and 74.9° correspond to the stainless-steel substrate. It clearly indicates the polycrystalline spinel ferrite films deposited on stainless steel substrates. In order to estimate the average size of crystallites for MFe_2O_4 in the films, the Scherrer equation [21] was used with the peak width of the (2 1 1) reflection for

Table 1
The optimized conditions for preparation of MFe_2O_4 (M = Cu, Ni and Co) films

Sample	Medium composition	Electrodeposition		Anodization	
		Current density (mA cm^{-2})	Time (min)	Current density (mA cm^{-2})	Time (min)
$CuFe_2O_4$	0.1 M $CuSO_4$ (15 ml) + 0.1 $MFeSO_4$ (5 ml)	2	12	10	20
$NiFe_2O_4$	0.1 M $NiSO_4$ (8 ml) + 0.1 M $FeSO_4$ (12 ml)	1.8	8	12	20
$CoFe_2O_4$	0.1 M $CoSO_4$ (7 ml) + 0.1 M $FeSO_4$ (13 ml)	1.8	10	10	20

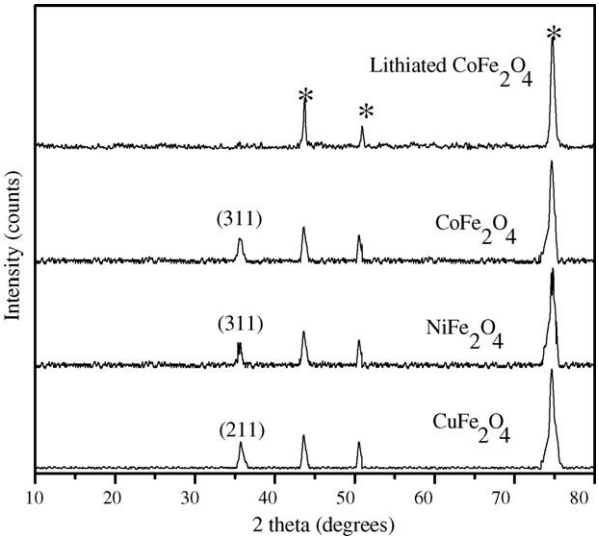

Fig. 1. X-ray diffraction patterns of MFe_2O_4 (M = Cu, Ni and Co) as-prepared films on the stainless-steel substrates and lithiated $CoFe_2O_4$ film firstly discharged to 0.01 V at a constant current of 10 μA cm^{-2}. The peaks of stainless steel substrate are marked with asterisks.

$CuFe_2O_4$, and (3 1 1) reflections for $NiFe_2O_4$ and $CoFe_2O_4$, respectively. The average crystallite sizes of MFe_2O_4 in the films were estimated to be about 50 nm taking a coefficient K to be 0.9.

Ex situ XRD measurements of lithiated MFe_2O_4 thin film electrodes were performed to examine the structure change after film electrode lithiation. As-prepared $CoFe_2O_4$ thin film electrode was firstly lithiated in the Li/$CoFe_2O_4$ film cell by discharge to 0.01 V at a constant current density of 10 μA cm^{-2}. As shown in Fig. 1, no other diffraction peaks except from the stainless steel substrate were observed for the lithiated $CoFe_2O_4$ film electrode, implying either the formation of an amorphous or nanostructured film with the particle size smaller that X-ray coherence length. The observed XRD patterns for the lithiated $CuFe_2O_4$ and $NiFe_2O_4$ film electrodes also showed no clear diffraction peaks. This behavior has also been observed in the powder electrodes of MFe_2O_4 (M = Cu, Ni, Co) [9,10] and $NiCo_2O_4$ [8].

Fig. 2(a–c) presents SEM images of the as-prepared $CuFe_2O_4$, $NiFe_2O_4$ and $CoFe_2O_4$ thin films on the stainless-steel substrate, respectively. It can be seen that these films consist of spherical particles with the average size of around 50 nm, although agglomeration is obvious especially for $NiFe_2O_4$ film. The cross-sectional view for the $CoFe_2O_4$ film on stainless-steel substrate is shown in Fig. 2(d) indicating that the prepared thin film is dense and smooth without any cracking, and the thickness of thin film is estimated to be about 300 nm.

The cyclic voltammograms (CVs) of $CuFe_2O_4$ and $NiFe_2O_4$ and $CoFe_2O_4$ thin films for the first three cycles at

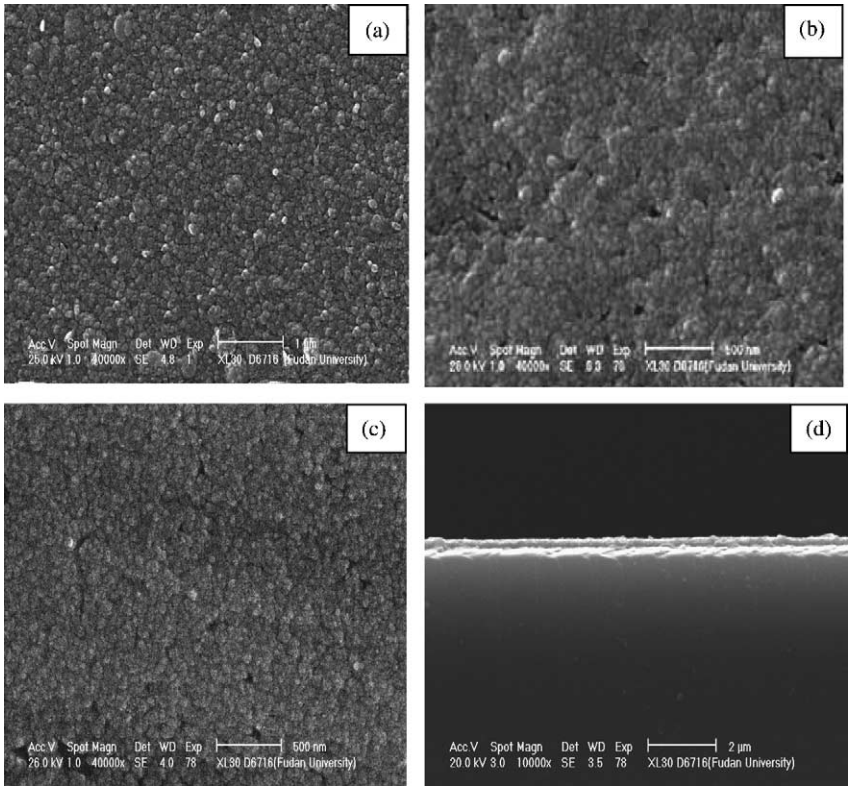

Fig. 2. SEM images of MFe_2O_4 prepared on the stainless-steel substrates: (a) $CuFe_2O_4$, (b) $NiFe_2O_4$, (c) $CoFe_2O_4$ (magnification is 1 × 40,000) and (d) SEM micrograph showing cross-sectional view of $CoFe_2O_4$ film.

a scan rate of 0.1 mV s^{-1} between 0.01 and 3.0 V are shown in Fig. 3(a–c), respectively. For these film electrodes, there is a substantial difference between the first and the subsequent cycles. In the first cycle, a large irreversible reduction peak A with a maximum at about 1.2 V, which disappears in the subsequent cycles. This peak could be associated with the irreversible reaction for electrolyte decomposition. A large cathodic peak B located at 0.7 V is probably associated with the reduction reactions of Fe^{3+} and M^{2+} with Li during the first discharge of MFe_2O_4 film electrodes. It is known that the first discharge plateau of Fe_2O_3 appeared at 0.7 V [22] and those of CoO, NiO and CuO were located at 0.5, 0.4 and 0.8 V [23], respectively. The reduction peaks of Fe_2O_3 and MO could be overlapped to form a broad cathodic peak B under our experimental conditions. The large anodic peak B′ appears at around 1.7 V for $NiFe_2O_4$ and $CoFe_2O_4$ and at 1.0 V for $CuFe_2O_4$, respectively. As we have reported that the anodic peak of $CoFe_2O_4$ film electrode prepared by PLD method was also located at the same voltage [11], and these anodic peaks could be attributed to the oxidation reactions of both metallic Fe and Co or Ni. However, the anodic peak B′ for $CuFe_2O_4$ appears at 1.0 V as shown in Fig. 3(a), which is as same as that in the first discharge curve of $CuFe_2O_4$ shown in Fig. 4(a). The electrochemical behavior of $CuFe_2O_4$ is different from $NiFe_2O_4$ and $CoFe_2O_4$ film electrodes, which could be due to the Cu(I) stability during the reduction of Cu^{2+} by lithium reported by Tarascon and co-workers [24]. In addition, it is well known that the shape of the CV profiles for thin film electrodes is very sensitive to the composition, morphology and thickness of film electrodes [25].

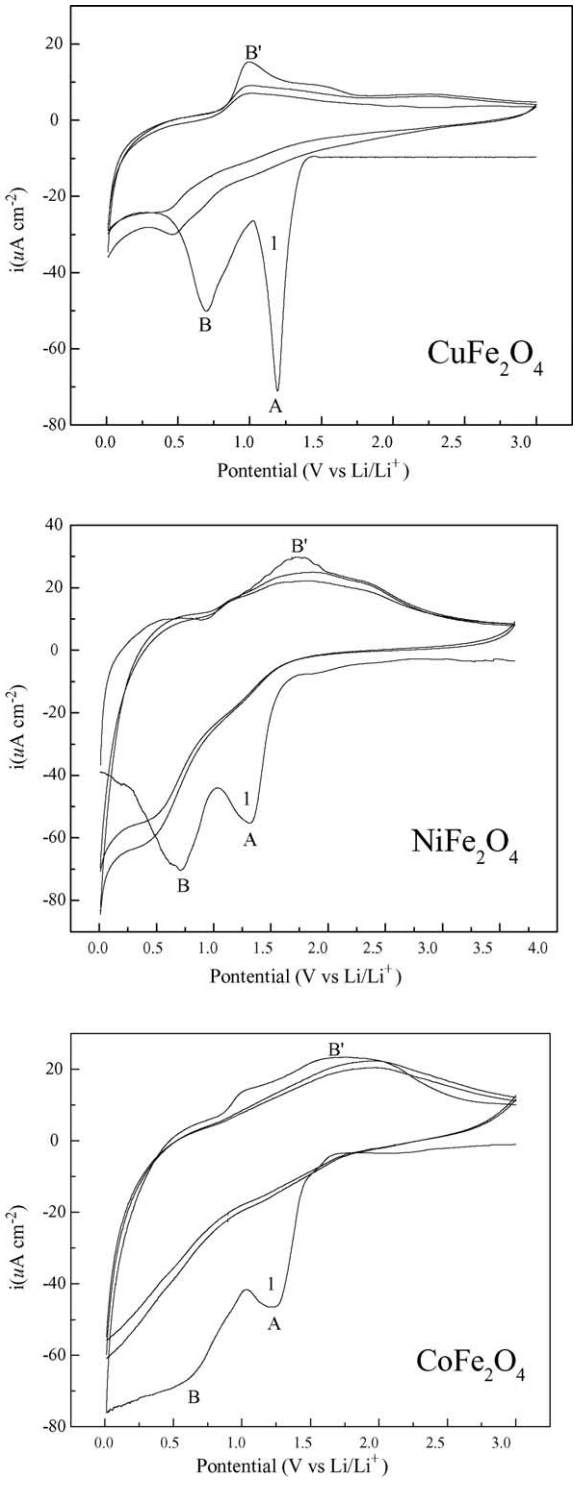

Fig. 3. CVs of $CuFe_2O_4$, $NiFe_2O_4$ and $CoFe_2O_4$ film electrodes for the first three cycles at a scan rate of 0.1 mV s^{-1}.

Fig. 4(a–c) displays the first three and 100th voltage–composition curves of $CuFe_2O_4$, $NiFe_2O_4$ and $CoFe_2O_4$ thin film electrodes between 0.01 and 3.0 V at a current density of 10 μA cm^{-2}, respectively. For three film electrodes, two plateaus appeared at 1.2 and 0.7 V were observed in the first discharge, and the voltages are close to those of CVs mentioned above. The plateaus in the subsequent reversible discharge curves are similar, but different from the first discharge which implies the occurrence of electrochemical Li-driven irreversible structure and textural change of the MFe_2O_4 thin film electrodes after the first discharge. For $CuFe_2O_4$ film electrode, the curve gives 6.72 Li per formula unit in the first discharge and only 4.03 Li can be reversibly removed, and the initial capacity loss is estimated to be 40%. It may be related to the morphology and textural changes of film electrode and irreversible reactions with electrolyte as the cell potential approaches 0.01 V. For $NiFe_2O_4$ and $CoFe_2O_4$ film electrodes, the same Li amount of about 4.02 per formula unit can be reversibly obtained with initial capacity loss of 35 and 32%, respectively.

The cycling performance of $CuFe_2O_4$, $NiFe_2O_4$ and $CoFe_2O_4$ thin film electrodes at a current density of 10 μA cm^{-2} is shown in Fig. 5. The corresponding electrochemical properties of those film electrodes are summarized in Table 2. For $CuFe_2O_4$ film electrode, an initial reversible capacity of 452 mAh g^{-1} was obtained and retained 75% of the capacity retention up to 100 cycles. $NiFe_2O_4$ and $CoFe_2O_4$ thin film electrodes exhibited the same initial reversible capacity of 460 mAh g^{-1}, and 77 and

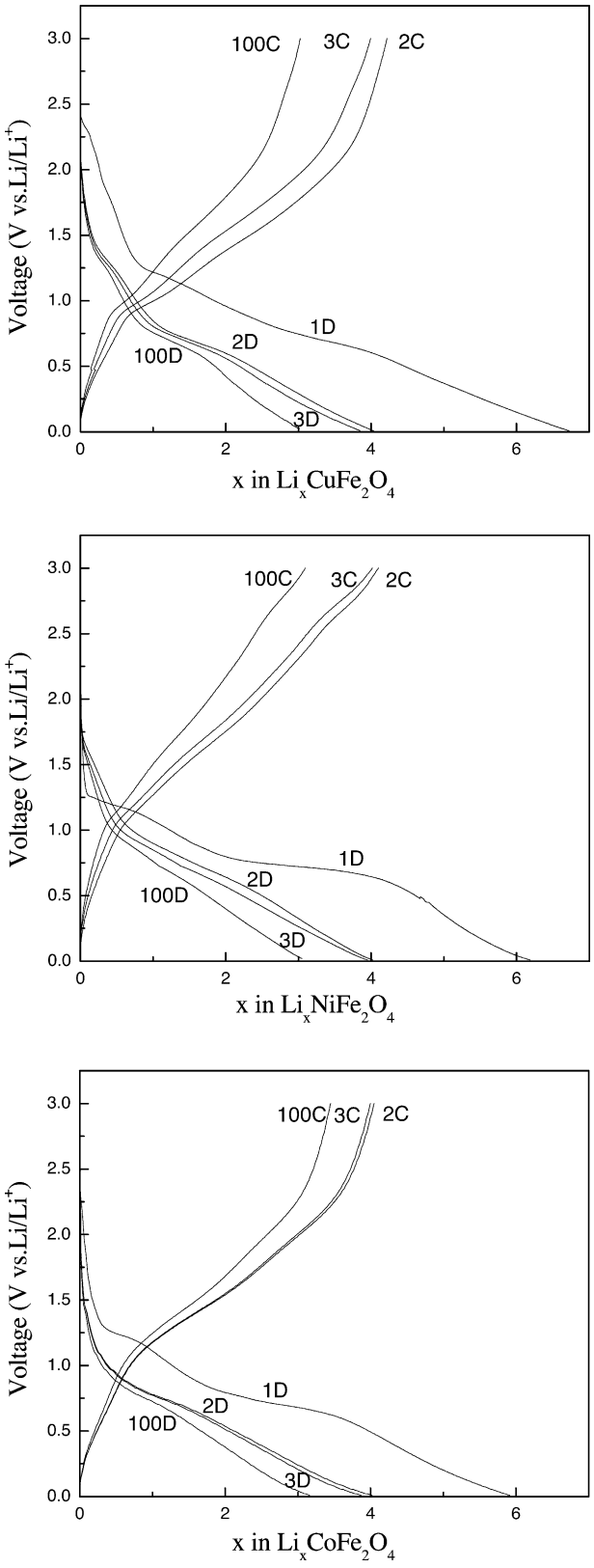

Fig. 4. The first three and 100th voltage–composition curves of MFe_2O_4 (M = Cu, Ni and Co) film electrodes between 0.01 and 3.0 V at a current density of 10 μA cm^{-2}. The *n*th discharge and charge are, respectively, denoted *n*D and *n*C.

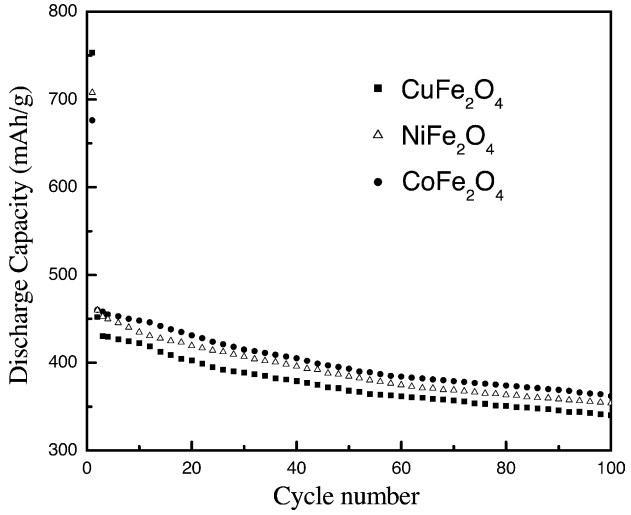

Fig. 5. Discharge capacity vs. cycle number for MFe_2O_4 (M = Cu, Ni and Co) film electrodes between 0.01 and 3.0 V at a current density of 10 μA cm^{-2}.

80% of the capacity can be maintained over 100 cycles, respectively. The cycling performance of $CoFe_2O_4$ thin film prepared in this work is not as good as that prepared by PLD method. It is most likely that PLD method can fabricate more strong adhesive films onto the substrate than the films made by the electrochemical route described in this paper.

The better electrochemical performance of MFe_2O_4 (M = Cu, Ni, Co) film electrodes comparing with their powder electrode counterpart [9,10] may be due to the fact that these film electrodes have nanocrystalline structure, and the thickness of these electrochemical active thin films is about 300 nm. It is well known that the spinel metal ferrites have very low electronic conductivity, which limits their electrochemical response for being used as an electrode material for Li-ion batteries. Striebel and co-workers have reported that very thin film might enhance electric conductivity from substrate and allow lithium ions to diffuse through the electrode more easily [26]. In addition, the nanostructure of film electrodes can reduce the lithium ion diffusion distance, improve diffusion kinetics and increase the particle size/volume effect on the reactivity of electrode material. But it should be noted that the nanocrytalline ferrite film electrodes suffer from a large capacity loss in the first cycle. This observed irreversible capacity not only arises from a conversion reaction of the nanocrystalline metal ferrite from M–O bond to Li_2O and the electrochemical driven formation of nanosized metallic grains, but also originates from the decomposition of the electrolyte and subsequent formation of an organic layer deposited on the film with a large surface area. Because of the complexity in determining the reaction mechanism of lithium with MFe_2O_4, further work will be done by using more advanced techniques in our laboratory.

Table 2
Electrochemical properties of MFe_2O_4 (M = Cu, Ni and Co) film electrodes

Film electrode	Initial reversible Li amount in MFe_2O_4	Initial capacity loss (%)	Initial reversible discharge capacity	100th discharge capacity	$R_{100/2}$ (%
$CuFe_2O_4$	4.03	40	452	340	75
$NiFe_2O_4$	4.02	35	460	355	77
$CoFe_2O_4$	4.02	32	460	365	80

$R_{100/2}$ is defined as the 100th/the second discharge capacity. MFe_2O_4 film/Li cells were cycled at 10 $\mu A\,cm^{-2}$ between 0.01 and 3.0 V. The unit of capacity is $mAh\,g^{-1}$.

4. Conclusions

Nanocrystalline transition metal ferrite MFe_2O_4 (M = Cu, Ni, Co) thin films have been prepared by an electrochemical route at room temperature. Electrochemical measurements showed not only $NiFe_2O_4$ film but also $CuFe_2O_4$ and $CoFe_2O_4$ films could be used as promising anode thin films for all-solid-state Li-ion batteries. The initial reversible capacity of MFe_2O_4 (M = Cu, Ni, Co) film electrodes reached 450–460 $mAh\,g^{-1}$ at a current density of 10 $\mu A\,cm^{-2}$ between 0.01 and 3.0 V, and remained about 75% of the reversible capacity up to 100 cycles. We suggested that the improved electrochemical performance of MFe_2O_4 film electrodes might result from the effect of nanosized structure of thin films on their electrochemical properties.

Acknowledgements

This work is supported by the National Nature Science Foundation of China (project no. 200083001). Authors thank professors Zheng-Wen Fu and Yan-Qiu Chu for their helpful discussions.

References

[1] M.M. Thackeray, J. Solid State Chem. 55 (1984) 280.
[2] J. Sarradin, A. Guessous, M. Ribes, J. Power Sources 62 (1996) 149.
[3] D. Larcher, C. Masquelier, D. Bonnie, Y. Chabre, V. Masson, J.B. Leriche, J.-M. Tarascon, J. Electrochem. Soc. 150 (2003) A133.
[4] J.J. Xu, G. Jain, Electrochem. Solid State Lett. 6 (2001) 190.
[5] P.N. Vasambekar, C.B. Kolekar, A.S. Vaingankar, Mater. Chem. Phys. 66 (1999) 282.
[6] C.D. Mee, Contemp. Phys. 8 (1967) 385.
[7] C.J. Chen, M. Greenblatt, Solid State Ionics 18–19 (1986) 838.
[8] R. Alcántara, M. Jaraba, P. Lavela, J.L. Tirado, Chem. Mater. 14 (2002) 2847.
[9] R. Alcántara, M. Jaraba, P. Lavela, J.L. Tirado, J.C. Jumas, J. Olivier-Fourcade, Electrochem. Commun. 5 (2003) 16.
[10] R. Alcántara, M. Jaraba, P. Lavela, J.L. Tirado, Electrochemical Society Meeting in Salt Lake City, Oral Communication, 131, 2002.
[11] Y.-Q. Chu, Z.-W. Fu, Q.-Z. Qin, Electrochim. Acta 49 (2004) 4915.
[12] Y.-N. NuLi, Y.-Q. Chu, Q.-Z. Qin, J. Electrochem. Soc. 151 (2004) A1077.
[13] H.J. Masterson, J.G. Lunney, D. Ravinder, J.M.D. Coey, J. Magn. Mater. 140–144 (1995) 2081.
[14] T. Tsuchiya, H. Yamashiro, T. Sei, T. Inamura, J. Magn. Magn. Mater. 27 (1992) 3645.
[15] M.F. Gillies, R. Coehoorn, J.B.A. VanZon, D. Aldern, J. Appl. Phys. 83 (1998) 6855.
[16] Z.J. Zhou, J.J. Yan, J. Magn. Magn. Mater. 115 (1992) 87.
[17] M. Naoe, N. Matsushita, J. Magn. Magn. Mater. 155 (1996) 216.
[18] D.M. Schleich, Y. Zhang, Mater. Res. Bull. 30 (1995) 447.
[19] S.D. Sartale, G.D. Bagde, C.D. Lokhande, M. Giersig, Appl. Surf. Sci. 182 (2001) 366.
[20] D. Guyomard, J.-M. Tarascon, J. Electrochem. Soc. 140 (1993) 3071.
[21] B.D. Cullity, Elements of X-ray Diffraction, second ed., Addison-Wesley, Reading, MA, 1978.
[22] D. Larcher, C. Masquelier, D. Bonnin, Y. Chabre, V. Masson, J.B. Leriche, J.-M. Tarascon, J. Electrochem. Soc. 150 (2003) A133.
[23] P. Poizot, S. Larnelle, S. Grugeon, J.-M. Tarascon, J. Electrochem. Soc. 149 (2002) A1212.
[24] S. Grugeon, S. Larnelle, R.H. Urbina, L. Dupont, P. Poizot, J.-M. Tarascon, J. Electrochem. Soc. 148 (2001) A285.
[25] A. Rongier, K.A. Striebel, S.J. Wen, E.J. Cairns, J. Electrochem. Soc. 145 (1998) 2975.
[26] S.-W. Song, K.A. Striebel, R.P. Reade, G.A. Roberts, E.J. Carins, J. Electrochem. Soc. 150 (2003) A121.